



Damage assessment in beam-like structures by correlation of spectrum using machine learning

Vien Le-Ngoc, Luan Vuong-Cong, Toan Pham-Bao*, Nhi Ngo-Kieu

Laboratory of Applied Mechanics (LAM), Faculty of Applied Science, Ho Chi Minh City University of Technology (HCMUT), VNU-HCM, Ho Chi Minh City, Viet Nam.

lvien.sdb19@hcmut.edu.vn, <http://orcid.org/0000-0002-8154-1014>

vuongluan@hcmut.edu.vn, <http://orcid.org/0000-0003-4146-9297>

baotoanbk@hcmut.edu.vn, <https://orcid.org/0000-0002-2105-2403>

ngokieuubi@hcmut.edu.vn, <https://orcid.org/0000-0001-9230-4308>

ABSTRACT. Damage assessment in the actual operating process of the structure is a modern and exciting problem of construction engineering due to several practical knowledge about the current condition of the inspected structures. However, the problem faced is the difficulty in controlling the excitation in structures. Therefore, the output-based structural damage identification method is becoming attractive because of its potential to be applied to an actual application without being constrained by the collection of the information excitation source. An approach of damage assessment based on supervised Machine Learning is introduced in this study by using the correlation of spectral signal as an input feature for artificial neural network (ANN) and decision tree. The output of machine learning algorithms consists of the appearance of new cuts, the level of cutting and the cutting position. A supported beam model was constructed as an experiment to determine if the method is reasonable for engineering structures. Two machine learning algorithms have been applied to check the relevance of the proposed feature from vibration data. This study contributes a standard in the damage identification problem based on spectral correlation.

KEYWORDS. Damage identification, Artificial neural network (ANN), Decision Tree, Spectral correlation, Beam-like structure.



Citation: Le-Ngoc, V., Vuong-Cong, L., Pham-Bao, T., Ngo-Kieu N., Damage assessment in beam-like structures by correlation of spectrum using machine learning, *Frattura ed Integrità Strutturale*, xx (2023) 300-319.

Received: 19.05.2023

Accepted: 14.06.2023

Online first: 20.06.2023

Published: 01.07.2023

Copyright: © 2023 This is an open access article under the terms of the CC-BY 4.0, which permits unrestricted use, distribution, and reproduction in any medium, provided the original author and source are credited.

INTRODUCTION

Structural health monitoring (SHM) and damage detection play a vital role in ensuring the safety and entirety of the structures by assessing the damage development and predicting the remaining life cycle of the structural systems such as buildings, dams and bridges, etc. It is a process in the experimental data as vibration response can be used to detect



and evaluate structural damage degrees appropriately. SHM process can be categorized into five levels [1]: (1) presenting damage, (2) localizing damage, (3) categorizing damage, (4) estimating damage severity, and (5) predicting the development of damage. As the main technique of SHM, structural damage detection has been intently applied for decades. Vibration signals are a popular big data source exploited to detect structural damage [2, 3]. These signals contain features that indicate sensitivity to structural damage. In the literature, vibration-based damage identification (VBDI) methods were investigated and applied in different structures such as trusses, frames, plates and beams [4]. Moreover, the beam is one of the useful elements in many large constructions. Therefore, the damage evaluation in the beams is also chosen in many studies about VBDI.

The traditional VBDI methods extensively use modal properties extracted from Fourier transform (FT) of response signals as natural frequencies, mode shape and damping [5]. Fourier transform is usually used to analyze signals in the time domain to Power spectral density (PSD) in the frequency domain. PSDs are also widely used in Structural Health Monitoring (SHM) [6-9]. Thus, the vibration features extracted in the frequency domain can be used for damage detection. However, these features are extracted from original vibrations. The types of vibration can influence each other and create deviations in properties. Or, specific properties will be hidden by other vibration mode properties. This may cause the monitoring and evaluation process to be inaccurate. Some inherent characteristics of the FT can affect damage detection accuracy. The FT loses the temporal information of the signals and cannot capture the evolutionary features in signals measured from naturally excited structures [10]. This makes FT challenging to detect damage and SHM.

A predictive model using Machine learning algorithms in the problem of damage identification has been proposed in many studies. Machine learning as neural network pattern recognition (NNPR) serves the damage detection process in beams [11-15] or conditional assessment in bridges [3, 16, 17]. Besides, machine learning methods are also applied in other structures, such as plates, pipes, and frames [18-20]. Nowadays, To increase the accuracy of machine learning algorithms, researchers usually combine machine learning with optimal algorithms such as the Whale optimization algorithm (WOA) for shear frame [21], the YUKI algorithm (YA) for metallic plates [22], and particle swarm optimization algorithm (PSO) for steel frame [23] to damage-sensitive input features. Thanh Cuong-Le et al. improved the input of the Support Vector Machine algorithm (SVM) by combining it with PSO, which is a method that can provide optimization features effectively for truss bridges and 3D frame structures [24]. In another way, Aman Grag et al. had to combine SVM with Gaussian Process Regression (GPR) to predict the compressive strength of concrete containing nano-silica [25]. The optimization methods are not only used in conjunction with the SVM algorithm but are also used with artificial neural networks (ANN) such as A. Ouladbrahim et al. used the Whale Optimisation Algorithm [26], or Muhammad Irfan Shirazi et al. used YUKI algorithm [19] to improve ANN inputs from that the performance of ANN is increased. Additionally, new machine-learning techniques have also been researched to increase the convergence speed during the process of training the network [27]. However, Analytical models are made when measurements are time-consuming and costly. Although many different models have been tested for many specific problems, a few models do not accurately predict because they depend on the particular condition. No unique model is suitable for the whole damage detection levels. The current situation is that the learning algorithms may not converge or have low accuracy on different data sets [28]. Hoshyar et al. showed that the SVM (support vector machine) model has the best performance of predictability and training time after testing nine machine learning models with real data to detect the existence of damage to concrete and reinforced concrete beam models in the laboratory [29]. Consequently, multi-step damage detection techniques are proposed to create each specialized machine learning model, making the SHM problem simple but achieving good results. Nazarko and Ziemiański proposed a two-step method consisting of 2 separate ANN prediction models to identify the damage location and existence with features such as wave amplitudes, spectral densities, and correlation factors [30]. That study shows that NN (Neural network) is very useful even when applied to complex signals such as elastic waves. The power spectrum depends on the mode shape of the vibration at different locations. In comparison to other locations, the shape of the power spectrum will be significantly different at the site of the damage. Therefore, the spectral correlation coefficient is used to evaluate the difference between the spectrum, helping to diagnose the damage. This study selects a combination of spectral density and correlation factors as the feature. In addition, a two-step algorithm is also proposed, with the first step being an ANN and the second being a decision tree. Decision trees provide a transparent and interpretable model with training speed and high computational efficiency. Decision trees are relatively faster to train than ANNs, especially when dealing with large datasets [31, 32]. The spectral correlation will be used to train machine learning with neural network pattern recognition (NNPR) for damage location and a decision tree for damage severity.



METHODOLOGY

Power spectral density of vibration

According to Euler–Bernoulli beam theory, the governing differential equation of beams is as follows:

$$A \frac{\partial^2}{\partial x^2} \left[EJ(x) \frac{\partial^2 u(x,t)}{\partial x^2} \right] + \rho \frac{\partial u^2(x,t)}{\partial t^2} + c \frac{\partial u(x,t)}{\partial t} = f(s,t) \tag{1}$$

where $u(x,t)$ is the displacement response of the beam in location x at the time t , EJ is bending rigidity, ρ is linear density, c is damping coefficient, and $f(s,t)$ is the external force in location s at time t . With singly supported beam, boundary and initial conditions are shown as follows:

$$\begin{aligned} u(0,t) = 0 \quad ; \quad u(l,t) = 0, \\ \frac{\partial^2 u(x,t)}{\partial x^2} \Big|_{x=0} = 0; \quad \frac{\partial^2 u(x,t)}{\partial x^2} \Big|_{x=l} = 0 \\ u(x,0) = 0 \quad ; \quad \frac{\partial u(x,t)}{\partial t} \Big|_{t=0} = 0; \end{aligned} \tag{2}$$

The solution of beam response with length L can be found in general forms as follows:

$$u(x,t) = \sum_{r=1}^{\infty} \phi_r(x) w_r(t) \tag{3}$$

in which $\phi_r(x)$ and $w_r(t)$ are r^{th} mode shape and r^{th} generalized displacement of the beam, respectively. From Eq. (1) and Eq. (3), the differential equation of the beam in each generalized coordinate is shown as:

$$\ddot{w}_r(t) + 2\xi_r \omega_r \dot{w}_r(t) + \omega_r^2 w_r(t) = f_r(t) \tag{4}$$

with ω_r , ξ_r and $f_r(t)$ are natural frequency, damping ratio and generalized force of r^{th} mode shape, respectively. This parameter is defined as

$$\rho \omega_r^2 \phi_r(x) = \frac{\partial^2}{\partial x^2} \left[EJ(x) \frac{\partial \phi_r(x)}{\partial x^2} \right] \tag{5}$$

$$\int_0^L \rho \phi_r(x) \phi_k(x) dx = \mu_r \delta_{rk} \tag{6}$$

$$\int_0^L c \phi_r(x) \phi_k(x) dx = 2\mu_r \omega_{nr} \xi_r \delta_{rk} \tag{7}$$

$$f_r(t) = \frac{1}{\mu_r} \int_0^L \phi_r(x) f(x,t) dx \tag{8}$$

with $H_r(\omega)$ is the frequency response function (FRF) of r^{th} mode shape, the vibration response of the beam can be found in the form as follows:

$$w_r(t) = \int_{-\infty}^{\infty} H_r(\omega) F_r(\omega) e^{i\omega t} d\omega \tag{9}$$



where $F_r(\omega)$ is the Fourier transform of force $f_r(t)$. The FRF of the beam at coordinate x by the load at coordinates s is determined as follows [33]:

$$H(x, s, \omega) = \sum_{j=1}^{\infty} \phi_j(x) H_r(\omega) \phi_j(s) \tag{10}$$

with $S_f(s, \omega)$ is the PSD of excitation at coordinate s , the PSD of the vibration response S_w is calculated as follows:

$$S_w(x, \omega) = S_f(s, \omega) \left| \sum_{r=1}^{\infty} \frac{\phi_r(x) \phi_r(s)}{(\omega_r^2 - \omega^2) + 2i\xi_r \omega_r \omega} \right|^2 \tag{11}$$

In general, PSD of response depends not only on material properties (natural frequency ω_n and damping ratio ξ) but also boundary conditions (mode shape ϕ). Doebling et al. [19] defined "damage" as the changes in a mechanical system's material characteristics or geometrical conditions. Therefore, the PSD of response will be variable by the presence and development of damage. According to S. Beskhyroun and T. Oshima [34, 35], a damage identification method using changes in the curvature of PSD is proposed and performed in a laboratory's numerical and experimental bridge models under fixed excitation. Then, dynamic measurements of a reinforced concrete beam have confirmed that the method is effective when it depends on the difference in the peak amplitude of PSD between undamaged and damaged beams [36]. The results show that these proposals increased the sensitivity of PSD in damage identification. Nonetheless, they should be considered to apply for real bridges because of random moving load. A damage index extracted from PSD of vibration response under traffic vehicles called the Loss Factor Function is used to monitor the material deterioration of the bridge [37, 38].

Damage sensitive feature

Correlation analysis has been a rarely-studied approach for damage identification because it concentrates on the relationship between two signals in the time domain. The Pearson correlation coefficient, developed by Karl Pearson (1880s) [39], is generally applied in estimating the relationship between two signals and has a value between -1 (inverse linear) and 1 (linear). A few studies used this coefficient to identify damage. For example, this coefficient is one of three techniques to analyze the relationship between the surface waveform for testing fatigue damage of reinforced concrete structural elements in Ref [40]. Two correlation coefficient-based algorithms were used for evaluating the ultrasonic wave to detect the interfacial damage of the coat-substrate structure [41]. A novel damage index based on the Pearson correlation coefficient is utilized ultrasonic-guided waves to detect damage in plate-like structures [42]. In addition, this coefficient was also used for correlation analysis together with transmissibility in the frequency domain between damage states and the baseline to detect damage to the benchmark structure [43]. In this study, the correlation between signals in the frequency domain as PSD of response at different positions in the mechanical system in the same condition is investigated changes of PSD when the system deteriorated. A measure of the similarity of two PSDs called the Power spectral correlation factor (PSCF) is defined as follows:

$$R_{S_i, S_j} = \frac{\text{cov}(S_i, S_j)}{\sigma_{S_i} \sigma_{S_j}} \tag{12}$$

where $\text{cov}(S_i, S_j)$ is the covariance between PSD $S_w(x_i, \omega)$ and PSD $S_w(x_j, \omega)$, σ_{S_i} and σ_{S_j} are standard deviations of PSD signal. Due to the positive-value characteristic of PSD, PSCF only takes values from 0 to 1.

Machine learning using neural network pattern recognition

Machine learning technology has been employed to verify the applicability of SHM, such as classification, regression, prediction and clustering. This study uses a machine learning method applied Artificial Neural Networks (ANNs) to classify damage. An ANN structure consists of several connected points arranged in different layers (Fig. 1).

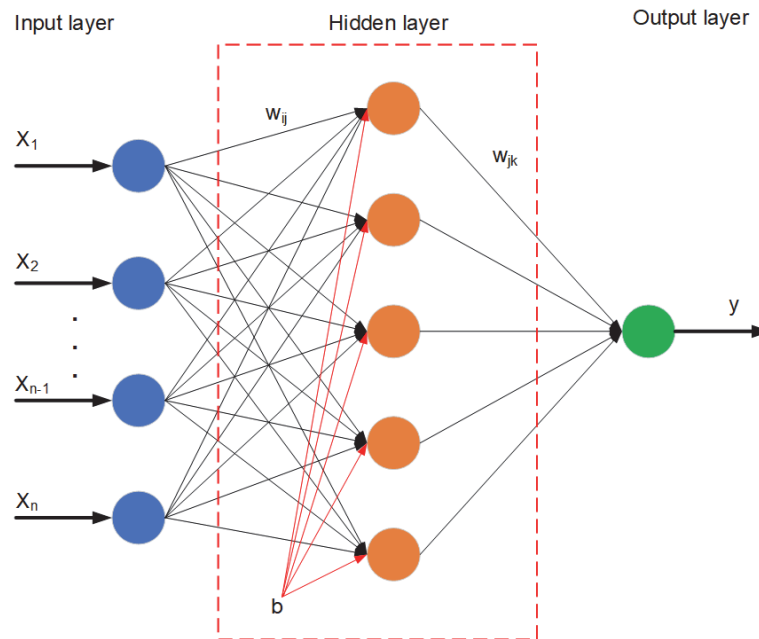


Figure 1: Simple neural network pattern recognition.

ANN is trained for damage identification in classification problems [44] and regression problems [45]. The non-parametric method allows for the slightest possible error in the recognition process. The training process improves performance (minimizing errors) using the back-propagation method to adjust the connection weights (w). In this neural network, the active function is a function of $u_k = \sum w_{ki}x_i + b_k$, where k is the k th neural order, and i th is the order of the i th input. Accordingly, the output of a neuron can be determined as follows:

$$o_k = f_k(u_k) = f_k\left(\sum w_{ki}x_i + b_k\right) \quad (13)$$

At the hidden layer, the value b_k (bias) is the regular selection to initialize the active function's value at each neuron due to the largest derivative of the error function. This makes the process of minimizing errors occur fast. The default error function of feed-forward networks is the average squared error (MSE). The MSE between the network output $o_k = f_k(u_k)$ and the target output $y_k(x)$ is defined as follows:

$$MSE = \sum_{k=1}^N \frac{(y_k - o_k)^2}{N} \quad (14)$$

Thus, the MSE is also a function dependent on u_k , and the rate of error improvement will be a derivative. Therefore, bringing u_k to the value whose derivative of the error function has the largest value makes the process of reducing errors faster because the rate of improvement of the error (the derivative of the error function) is initialized with the most significant value.

Machine learning using Decision Tree algorithm

In machine learning, classification and regression are two-step processes consisting of learning and prediction steps. The learning step involves developing a model based on training data, and the prediction step consists in using the model to predict data response. Decision trees (Fig. 2) are a popular machine-learning algorithm for classification and regression tasks [46, 47]. They allow complex relationships between input features and output targets to be modelled in an easy-to-use but assertive manner.

A hierarchical tree structure consists of root nodes, branches, internal nodes, and leaf nodes. In a decision tree, each node represents a decision, and branches that emanate from the root node are fed into internal nodes called decision nodes. At the end of each branch, terminal or leaf nodes represent the predicted outcome of the decision process. The algorithm constructs the decision tree based on a training dataset by selecting the most relevant features. Feature selection begins at



the root node and moves down the tree, then select the next feature with the most excellent predictive power. Depending on the selected features, the algorithm recursively splits the data into smaller subsets until all or most records can be classified.

One of the decision tree types is the bagged decision tree algorithm, also known as bootstrap aggregating, which is an ensemble learning method that combines multiple decision trees to improve the accuracy and stability of predictions [48]. In the algorithm, the training data is randomly sampled with replacement to create multiple bootstrap samples, and each is used to grow a separate decision tree [49]. The algorithm aims to improve the performance and accuracy of decision trees by reducing the variance and overfitting. After aggregating the predictions of each decision tree, the ensemble's final prediction is determined.

The bagged decision tree works as follows:

- Bootstrapping.
- Decision Tree Construction.
- Prediction Aggregation.

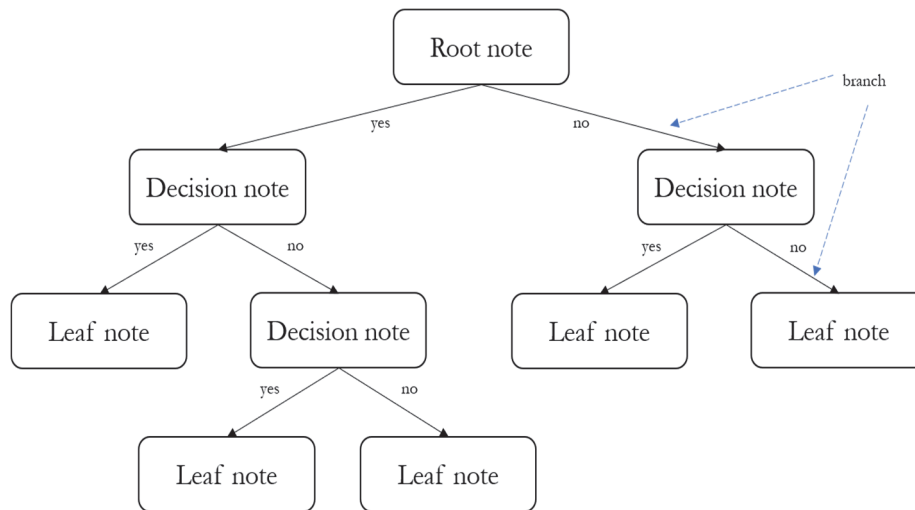


Figure 2: The decision tree diagram.

Proposed method

Damage identification is a multi-level problem: detecting, locating, assessing damage, etc. The first stage uses methods for the location of damage in the structure. This level can be performed without previous information on the system response when it is damaged. These methods are called novelty detection [50]. Later-stage damage detection methods provide information on the assessment of the damage. The pattern recognition approach can be used if there are large amounts of data in both computational and experimental investigations. Training a neural network pattern recognition for damage identification makes tracking the vibration signal simpler. To achieve the best recognition process features sensitive to damage are used as the inputs of ANN. These features are exploited by analyzing changes in the PSD corresponding to the weakening of the structure. For promising results in applying SHM [45, 51-53], Matlab software with many training algorithms available in Neural Network Toolbox is used in this paper to map features as PSCFs to damage levels. The Levenberg-Marquardt back-propagation algorithm is chosen because of its good performance on function fitting (nonlinear regression) problems [30, 45]. Additionally, we implement a decision tree algorithm to classify the level of cuts through the reworked PSCFs.

A good SHM process must be able to evaluate all damage levels. However, damage identification is only possible when the damage's presence and severity change the structural responses. Therefore, in this study, the appearance and the severity of damage are the targets of the network. The stiffness of the damaged section shows the severity of the damage. A two-level VBDI process (Fig. 3) is proposed to signal the presence of damage and assess severity. All input parameters for the network are calculated based on scenarios of damage levels. However, the study trained two machine learning algorithms for damage location and severity estimation to recognize samples obtained from slightly damaged models in the laboratory.

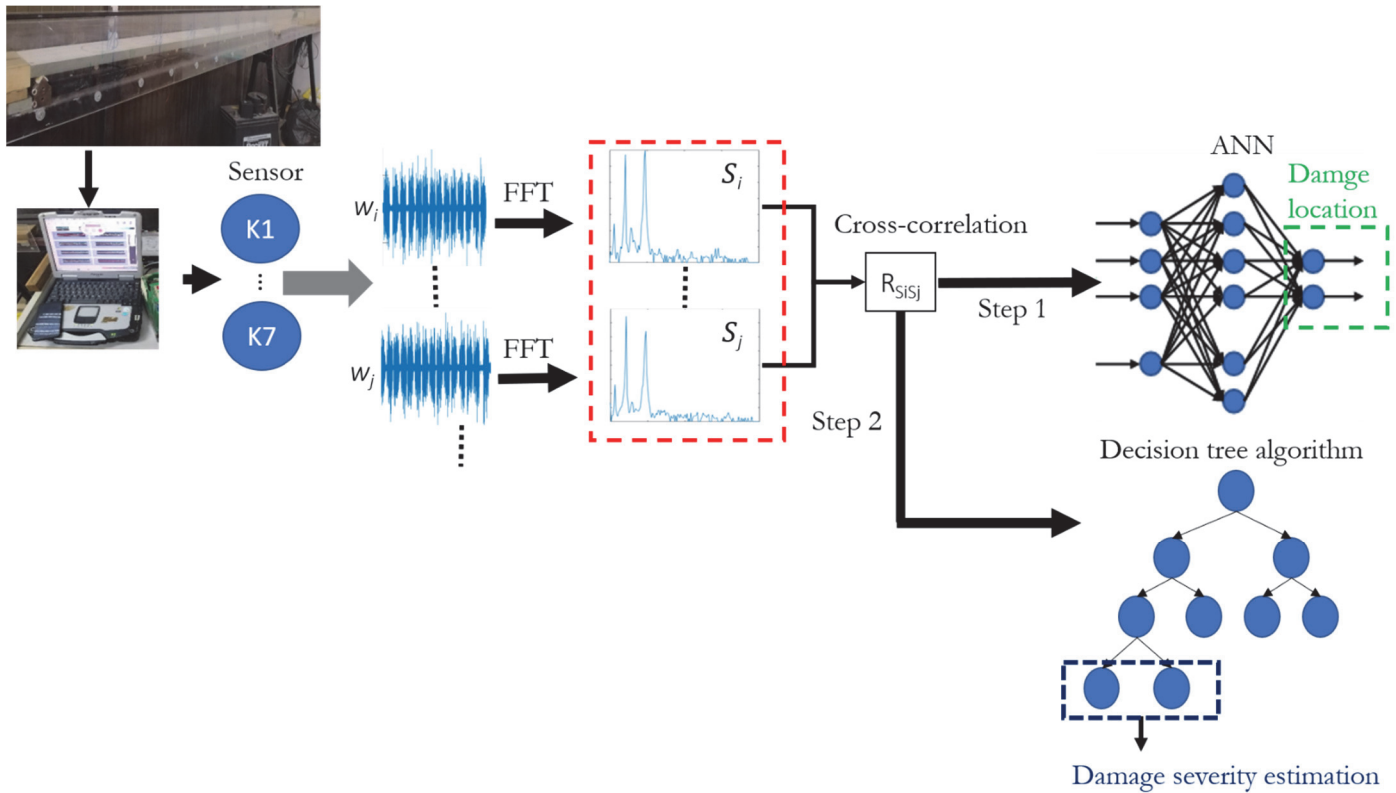


Figure 3: Schematic representation of proposed methodology.

FFT is applied to convert the acceleration signal into an amplitude-frequency spectrum, and then features suitable for damage identification are calculated from the measurement of the vibration signals at scenarios. After that, the first-level identification is performed by the ANN trained for novelty damage detection. If the presence of damage occurs, the second-level identification will be carried out using the decision tree trained to assess the level of the damage. The resulting output vector will evaluate the extent of the damage.

EXPERIMENT MODEL AND FEATURE EXTRACTION

Experiment model

The study experimented with a wooden beam supporting two ends as a model for an actual bridge girder. Wooden beams have a set of dimensions length \times width \times thickness of 1.2 m \times 0.1 m \times 0.017 m. The load moving on the beam is implemented to collect a large number of vibration signals of the beam through different beam states for evaluation. This test applies a moving load to a wooden beam by a motor driving a moving load of 3 kg. The inverter controls the vehicle's speed in the frequency range from 20Hz to 50Hz, equivalent to 37.7cm/s to 94.25 cm/s. According to the frequency values of the inverter, we denote these velocities as V1 to V16, as shown in Tab. 1. This experiment then uses seven accelerometers (K1, K2, K3, K4, K5, K6, K7) to measure the acceleration at seven positions: 1/8, 2/8, 3/8, 4/8, 5/8, 6/8, and 7/8, along the beam length.

There are twelve scenarios for the structural condition of beams: intact (undamaged) and eleven damaged states with different damage locations. Initially, we measured the vibration of the intact beam. We then make a cut near the 4th sensor position (K4) and continue to perform vibrations to capture data. Then we continue to increase the depth of the cut by three more cases. Cuts were made at positions near the 1st sensor (K1) and the 7th sensor (K7), respectively. Cuts are made with a constant width of 0.006 m, a depth which is increased to 0.003 m, 0.006 m, 0.009 m, and 0.011 m, respectively, extending the entire beam width. Seven accelerometers are installed under the beam along the length of the beam to collect the signal. Each accelerometer sensor records continuously for 400 seconds under each speed state during a recording period of 10 s with a sampling frequency of 2000. Data is recorded 12 times for 12 different beam scenarios. We used speeds from V1 to V16, shown in Tab. 1, to create a data bank. Its test model and actual implementation are illustrated in Fig. 4 and Fig. 6, and the shape of the cuts is shown in Fig. 5. The 12 damage situations are listed in Tab. 2, and the accelerometer sensor



specifications are shown in Tab. 3. Finally, some measured acceleration signals of structural conditions are presented in Fig. 7.

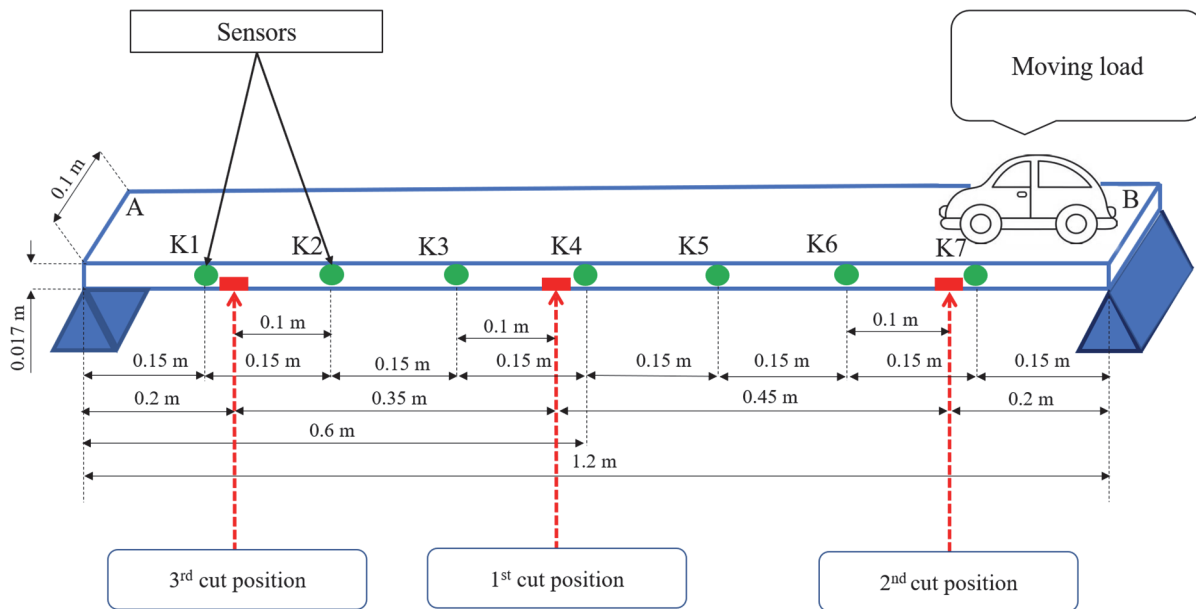


Figure 4: Illustrate the experiment model.

Symbol	Velocity (cm/s)
V1	37.7
V2	41.47
V3	45.24
V4	49.01
V5	52.78
V6	56.55
V7	60.32
V8	64.09
V9	67.86
V10	71.63
V11	75.4
V12	79.17
V13	82.94
V14	86.71
V15	90.48
V16	94.25

Table 1: Speed and mass of the moving load (load mass: 3 kg).

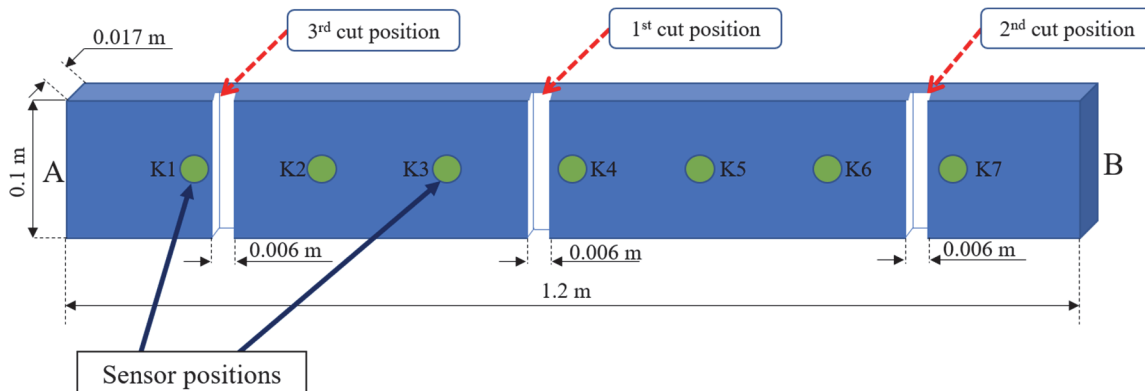


Figure 5: The shape of the cuts.

Damage state (symbol)	Quantity of damage	Location of damage		
		1 st Cut (depth)	2 nd Cut (depth)	3 rd Cut (depth)
H00 (Intact Beam)	0	-	-	-
H01	1	Nearly K4 (3mm)	-	-
H02	1	Nearly K4 (6mm)	-	-
H03	1	Nearly K4 (9mm)	-	-
H04	1	Nearly K4 (11mm)	-	-
H05	2	Nearly K4 (11mm)	Nearly K7 (3mm)	-
H06	2	Nearly K4 (11mm)	Nearly K7 (6mm)	-
H07	2	Nearly K4 (11mm)	Nearly K7 (9mm)	-
H08	2	Nearly K4 (11mm)	Nearly K7 (11mm)	-
H09	3	Nearly K4 (11mm)	Nearly K7 (11mm)	Nearly K1 (6mm)
H10	3	Nearly K4 (11mm)	Nearly K7 (11mm)	Nearly K1 (9mm)
H12	3	Nearly K4 (11mm)	Nearly K7 (11mm)	Nearly K1 (11mm)

Table 2: Scenarios of structural condition.

Parameter	Magnitude
Rated capacity	$\pm 19.61 \text{ m/s}^2 (\pm 2G)$
Nonlinearity	Within $\pm 1\%$ RO
Hysteresis	Within $\pm 1\%$ RO
Rated output	0.5 mV/V (1000×10^{-6} strain) or more
Safe temperature	-15 to 65°C
Safe excitation	6V AC or DC
Recommended excitation	1 to 3V AC or DC
Input resistance	$121\Omega \pm 1.7\%$
Output resistance	$121\Omega \pm 1.7\%$
Cable	4-conductor (0.08mm^2) vinyl shielded cable, 3.2mm diameter by 5m long
Safe overload	300%
Frequency response	DC to 60Hz $\pm 5\%$
Transverse sensitivity	4% RO or less
Weight	Approx. 25g (excluding cable)

Table 3: Specifications of accelerometers.

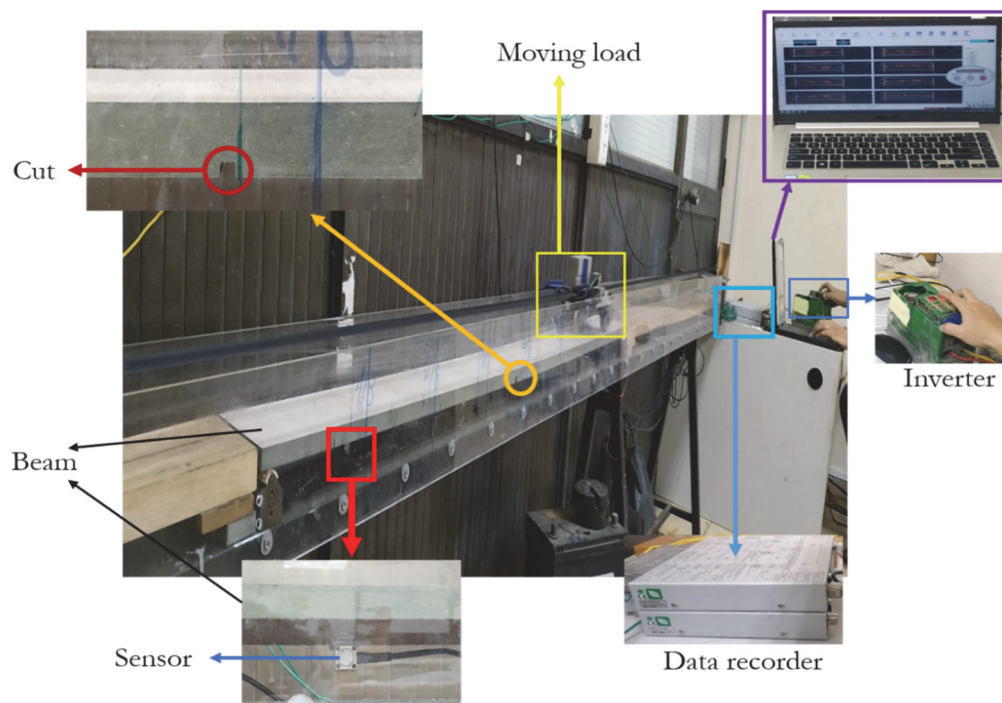


Figure 6: Deployment in the laboratory.



Feature extraction

Using vibration signal analysis, researchers can study the frequency components of a mechanical system by measuring its vibration response to external stimuli or internal forces. The spectrum of a vibration signal provides valuable information about the mechanical behaviour of the system, including its natural frequencies, damping ratios, and mode shapes. Spectrum analysis is a powerful tool in signal processing that allows us to understand a signal's sinusoidal components at different frequencies. By performing a Fourier transform on a signal, it is possible to determine its spectrum. The spectrum can provide insights into the underlying physical processes that generate the signal.

Additionally, the spectral analysis of the vibration signal can identify anomalies or defects in the system by analyzing the frequency response number of a structure for external forces. Furthermore, researchers can obtain information about its stiffness and damping properties to evaluate structures' performance and safety. Therefore, we use the spectrum in this study to look for the sensitive feature.

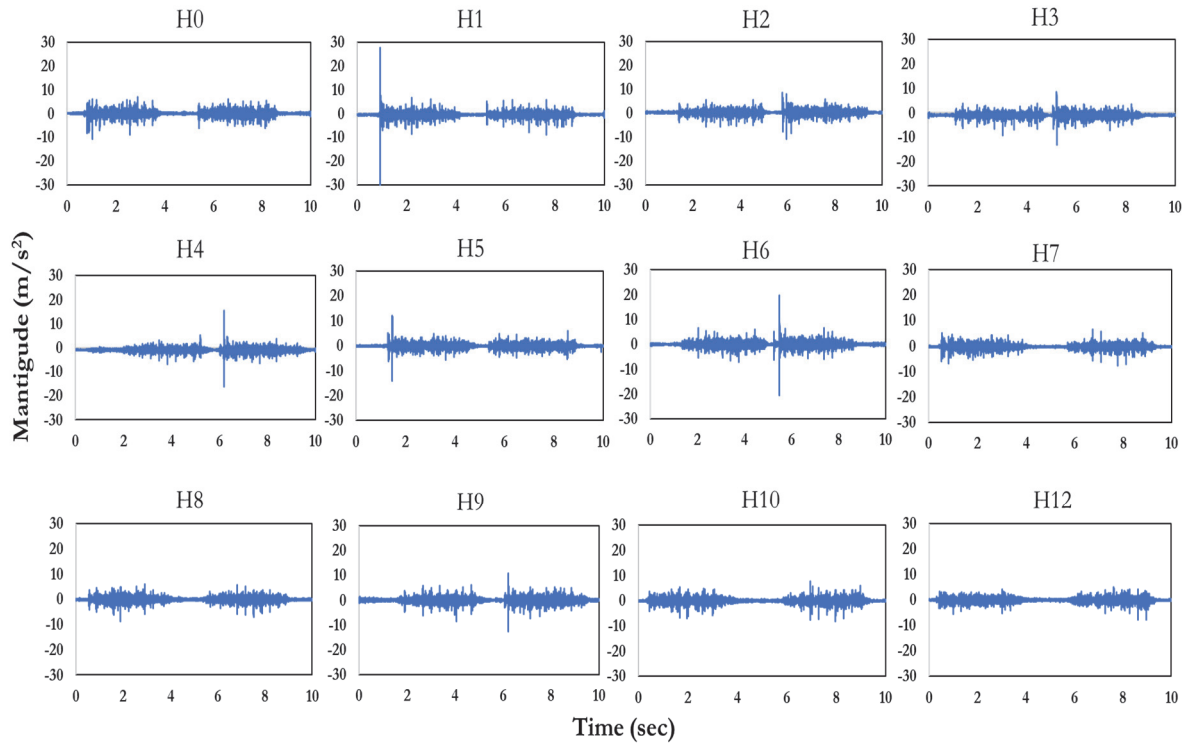


Figure 7: Original signal of twelve states.

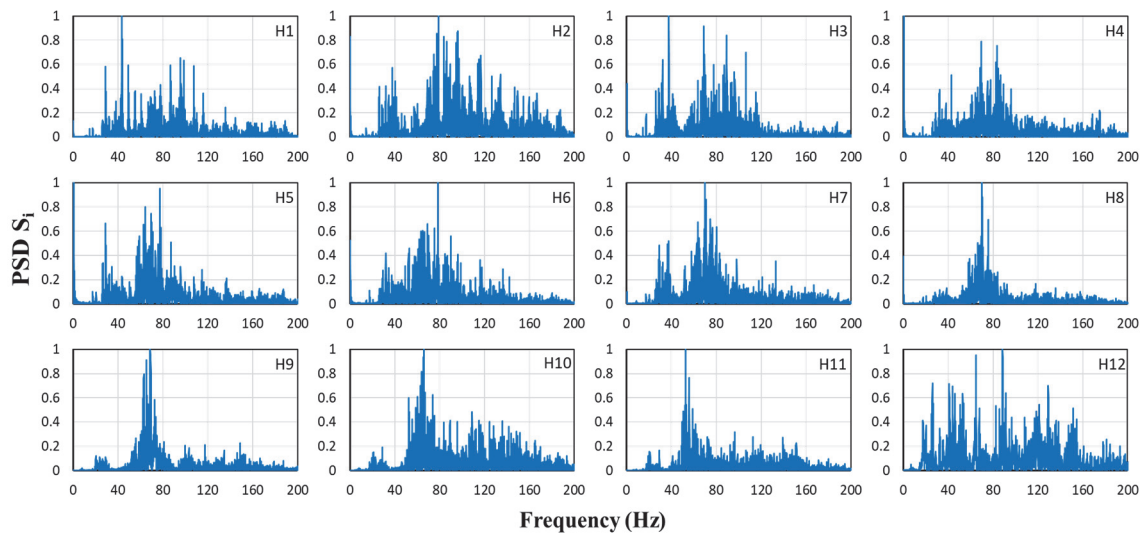


Figure 8: The spectrums of twelve states.

Specifically, each acceleration signal (10s) will be converted into a separate amplitude-frequency spectrum for feature extraction, as shown in Fig. 8. Several studies have indicated that exploiting damage-sensitive features in the frequency domain will accurately describe the system's properties. Consequently, tracking natural frequency changes is recommended in many studies for damage diagnosis. This study uses the correlation coefficient according to Eq. (12) to evaluate spectra evolution through different scenarios.

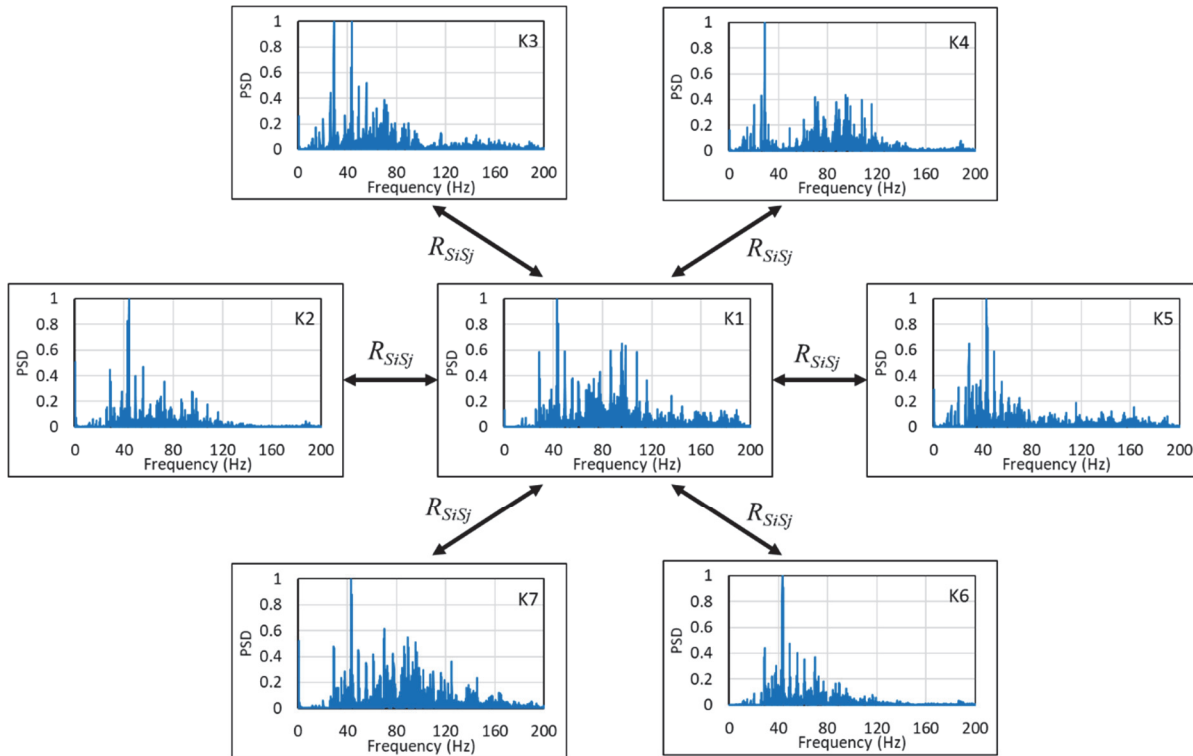


Figure 9: Spectra of measurement locations(sensors) and the procedure for calculating correlation values.

To create a feature by correlation of spectral value, we calculate the value of spectral correlation between measurement locations. Specifically, as shown in Fig. 9, we calculate the correlation of the spectral value of sensor K1 with other spectral values (K2, K3, K4, K5, K6, K7). Similarly, implementing the calculation for all measurement locations, we obtain a 7×7 matrix, including the correlation values shown in Tab. 4.

	K1	K2	K3	K4	K5	K6	K7
K1	1	0.62213	0.66153	0.68644	0.65229	0.56469	0.63889
K2	0.62213	1	0.98656	0.95169	0.98866	0.10808	0.99479
K3	0.66153	0.98656	1	0.96307	0.98438	0.18497	0.98252
K4	0.68644	0.95169	0.96307	1	0.95504	0.13951	0.95849
K5	0.65229	0.98866	0.98438	0.95504	1	0.20295	0.98748
K6	0.56469	0.10808	0.18497	0.13951	0.20295	1	0.14909
K7	0.63889	0.99479	0.98252	0.95849	0.98748	0.14909	1

Table 4: Correlation coefficient of the spectrum between measurement sites.

We remove the duplicate or similar correlation coefficient values and only take the distinct values. Therefore, the remaining data have 21 correlation values, as shown in Fig. 10.

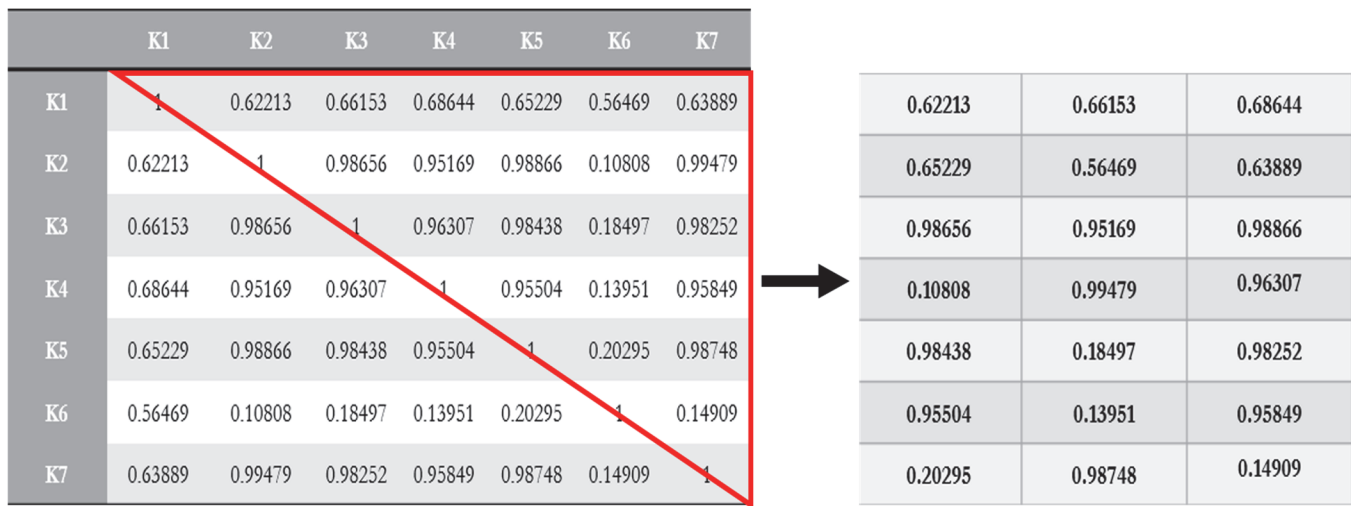


Figure 10: Feature extraction from correlation values.

H00	H01	H02	H03	H04	H05	H06	H07	H08	H09	H10	H12
0.60373	0.98984	0.98138	0.94406	0.18671	0.2043	0.89285	0.97967	0.9483	0.8603	0.91367	0.70168
0.62988	0.99112	0.82868	0.99916	0.99903	0.9704	0.36569	0.91765	0.2694	0.37969	0.36616	0.60782
0.67609	0.23272	0.98526	0.99942	0.99976	0.9979	0.4139	0.52718	0.89601	0.7493	0.78573	0.54059
0.64161	0.98952	0.9808	0.99941	0.9997	0.9973	0.38231	0.23169	0.82499	0.65797	0.60292	0.50153
0.53629	0.98895	0.98458	0.999	0.99958	0.99665	0.35978	0.28321	0.28277	0.25739	0.29858	0.54216
0.62444	0.9899	0.98133	0.91379	0.99967	0.99669	0.35949	0.91806	0.56208	0.47793	0.54146	0.60158
0.98803	0.99963	0.77774	0.94412	0.19309	0.31786	0.42524	0.89244	0.38849	0.39025	0.39288	0.53269
0.94818	0.13292	0.99935	0.94323	0.18474	0.19541	0.45957	0.54044	0.89621	0.79191	0.75319	0.4905
0.98548	1	0.99999	0.93702	0.16704	0.14894	0.44028	0.24574	0.74418	0.53269	0.50915	0.23078
0.09548	0.98569	0.9766	0.94603	0.18644	0.13465	0.41641	0.33623	0.35687	0.32182	0.33884	0.64655
0.99499	1	0.99999	0.9409	0.16388	0.13484	0.41586	0.89227	0.60204	0.5542	0.56225	0.5639
0.95804	0.14856	0.7887	0.99864	0.99896	0.96766	0.9976	0.20066	0.43113	0.49841	0.45912	0.47899
0.98394	0.99957	0.77595	0.99929	0.99893	0.96685	0.99928	0.010571	0.33086	0.53437	0.56324	0.59767
0.16515	0.98783	0.83766	0.99902	0.99909	0.96311	0.99988	0.10415	0.59569	0.52507	0.48101	0.44425
0.98515	0.99961	0.7771	0.91038	0.99875	0.96308	0.99986	0.99997	0.55827	0.43137	0.5416	0.5797
0.95169	0.13117	0.99928	0.99866	0.99947	0.99505	0.99767	0.52337	0.7279	0.5876	0.59223	0.21196
0.13319	0.20682	0.97874	0.99862	0.99942	0.9946	0.99729	0.49814	0.33009	0.32595	0.37895	0.32652
0.95599	0.13338	0.99936	0.91905	0.99946	0.99467	0.99728	0.20103	0.57706	0.49552	0.5639	0.44114
0.21423	0.98535	0.97608	0.99884	0.99951	0.99959	0.99905	0.57139	0.3786	0.41179	0.53938	0.40747
0.98593	0.99999	0.99999	0.90457	0.99996	0.99959	0.99902	0.009356	0.53647	0.43314	0.61867	0.53455
0.14253	0.98586	0.97676	0.92035	0.99941	1	1	0.10294	0.7017	0.58701	0.80632	0.73129

Table 5: The correlation values of twelve damage scenarios.

Since the signal is received continuously for 400s, we will have 40 amplitude-frequency spectrums with the same velocity. Therefore, with 16 speeds and 12 damage scenarios, we will have $16 \times 40 \times 12 = 7680$ spectrums. Finally, we obtain a data bank of 7680 samples, each including 21 spectral correlation values.

According to formula (11), the power spectrum at locations on the structure depends on the mode shape. The shape of the power spectrum will vary significantly at the damage location compared to the other location. Therefore, the cross-correlation calculation will show the difference in spectral shape. From that, it is possible to detect the appearance and location of damages. The data sample for the correlation coefficient results of twelve scenarios is shown in Tab. 5. Although it is clear that the correlation values are different, we cannot evaluate this difference through basic techniques. Therefore, we decided to use machine learning for damage assessment.



ANN STRUCTURE AND APPLYING ANN, A DECISION TREE FOR DAMAGE DETECTION

ANN structure and training process

The mechanical properties of the structure change due to the appearance of damage or weakening of the structure, and the vibration spectral characteristics can provide valuable information about the properties and behaviour of the structure through the change of spectrum. As conventional methods are labour-intensive, machine learning methods are superior in assessing these related changes. Therefore, machine learning methods are nominated in this paper. We use an ANN to detect and locate the cut, then use the decision tree algorithm to evaluate the level of the cuts. Due to machine learning tools, identifying and locating the appearance of damage or cuts becomes more straightforward and more precise. However, feature extraction is essential in achieving ANN or decision trees with high accuracy and generalization ability. This study extracts damage-related sensitive features from spectral correlations between measurement locations to identify damage-related sensitive features.

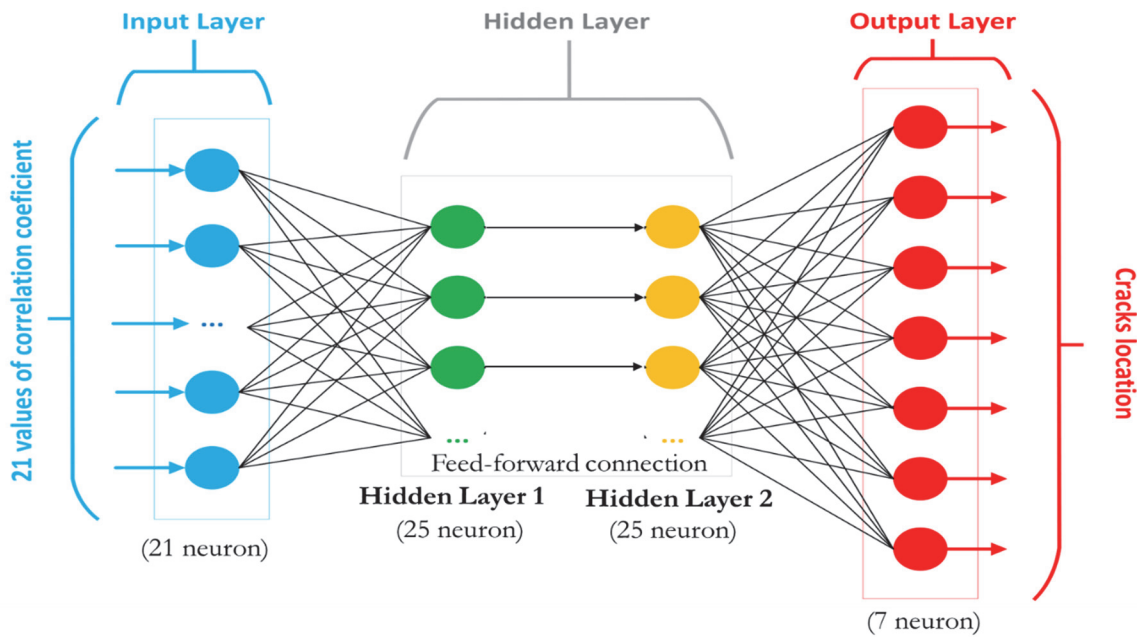


Figure 11: Architecture of the proposed feed-forward neural network.

The proposed ANN has one input layer, two hidden layers and one output layer (Fig. 11). The input layer is the spectral correlation values, totalling 21 features. According to the last experience, the number of hidden neurons should be 2/3 the size of the input layer plus the size of the output layer. Therefore, with 21 inputs and 7 outputs, we estimate around 20-25 neurons in hidden layers. The features are then fed into two layers, with 25 neurons in each layer. These classes use a log-sigmoid transfer function (logsig), whose expression is as follows:

$$\text{logsig}(n) = \frac{1}{1 + e^{-n}} \quad (15)$$

Terminally, the output layer consists of seven neurons with values 0 to 1 for damage detection. The activation function in the output layer is a hyperbolic tangent sigmoid transfer function (tansig) with the following formula:

$$\text{tansig}(n) = \frac{2}{1 + e^{-2n}} - 1 \quad (16)$$

These outputs will have a value from 0 to 1 to indicate the presence or absence of damage. We assume that the beam has damage (a cut or more) when the output value is approximately one and no damage when the output is around 0. Additionally, these seven values correspond to the sensors K1 to K7 along the beam length to determine the damage



location. To interpret the ANN model's results, we analyzed each neuron's output values to determine the most likely type of damage. If the first neuron has a value of around one and all other neurons have nearly 0, we conclude there is damage at the first sensor site (K1). If there is more than one damage, the value approximately equal to 1 of the ANN's output will be increased. In general, by analyzing the output values of 7 neurons in the ANN model, we can interpret the probability of appearance and location of damage in different damage scenarios.

The databank from the experiment, which contains 6912 samples (90% of the data bank) for eleven damage and integrity scenarios, is employed to train the proposed ANN architecture. This databank is split into three fractions for training, validation, and testing with ratios of 80%, 10%, and 10%, respectively. The maximum number of epochs for training is set up to 100. However, a validation criterion also comes into effect to stop the training process. The training process will be stopped when the number of consecutive failures is 6 in the validation. The training process employs the Levenberg-Marquardt back-propagation to update the weights and biases. The training process of the ANN was finished at the 47th epoch because it met the validation criterion. The best validation performance is attained at the 41st epoch, as shown in Fig. 12.

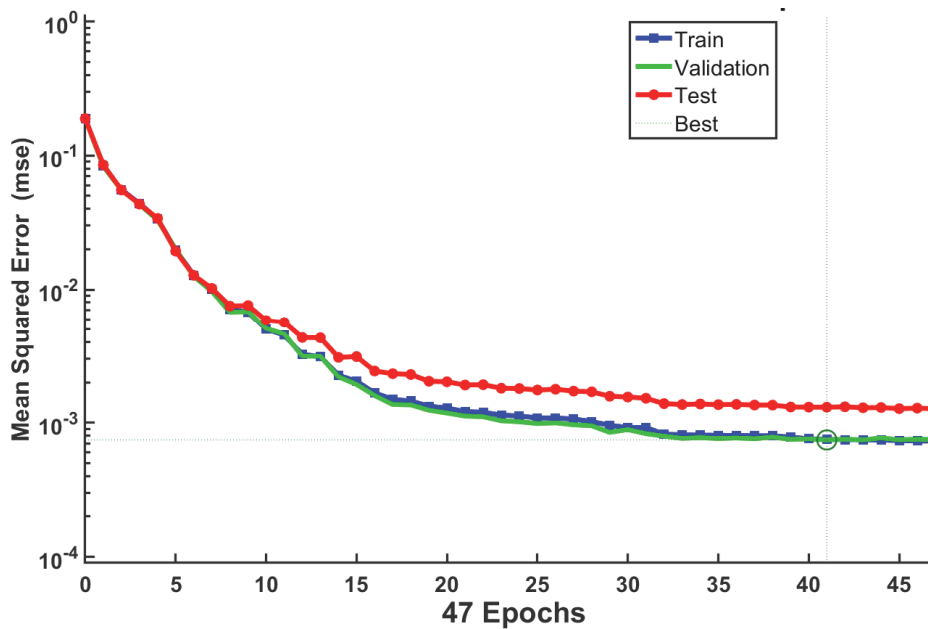


Figure 12: Training performance of the proposed neural network (best Validation Performance is 0.00074464 at epoch 41).

Applying ANN for damage identification and location

In order to confirm the generality of trained ANNs, this study uses 764 samples to test. These samples are extracted from the experimental data (10% of the data bank) and not used for training. Because of the large number of samples used for testing, we present the test results with ten representative samples for each damage state, as shown in Fig. 13.

As observed in Fig. 13, all predictions of ANN for ten samples are correct in different states. Although some samples of beams with cuts give a value not close to 1, their probability is still greater than 0.5. The results show that the trained ANN reaches remarkable generalizability. With ten samples for each damage scenario, most of the predictions of the proposed ANN are correct. Only some did not achieve the desired value when predicting the location of the second and third cuts. The proposed method is highly feasible for potential applications based on these results.

Application of the decision tree method to assess the extent of the cuts

In structural health monitoring, detecting and locating damage is essential, and determining the extent of damage is equally important. Therefore, in this paper, we propose to use a decision tree to evaluate the damage level based on the spectral correlation coefficient.

The bagged decision tree algorithm is a machine learning technique that has gained popularity due to its advantages over ANN. The algorithm produces decision trees that are easy to interpret and explain. Tree structures can be used to visualize decision trees, making it easier to understand how the model arrived at specific predictions. In addition, a major advantage of the algorithm is that it can be parallelized, so multiple decision trees can be trained simultaneously, significantly reducing

the training time compared to an ANN algorithm. Therefore, we choose the bagged decision tree algorithm despite ANN to assess the extent of the cuts.

This study used TreeBagger's supervised machine learning function in Matlab software to analyze and model the extracted feature data. In this implementation, we use a dataset including 6338 samples and train a TreeBagger model with 50 trees. Fig. 14 shows a decision tree made up of the training dataset. We then compute the model's out-of-bag (OBB) error, which estimates the classification error on new data. We use 702 samples, including 11 damage scenarios, to test the reliability of the decision tree. The results are represented by the confusion matrix shown in Fig. 15.

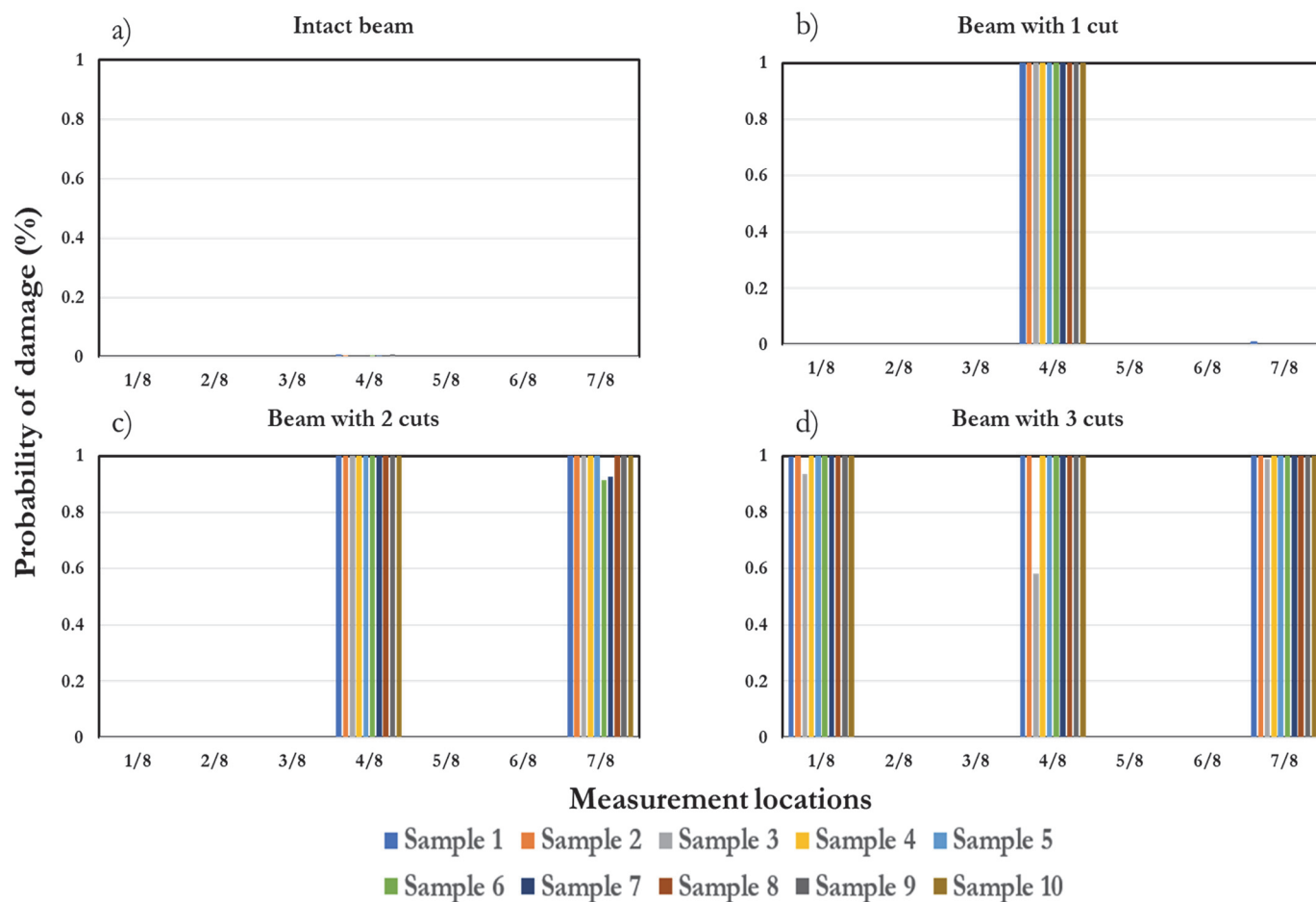


Figure 13: Output of the proposed ANN for damaged locations: a) Intact beam; b) Beam with one cut at 4/8 position; c) Beam with two cuts at 4/8 and 7/8 position; d) Beam with three cuts at 1/8; 4/8 and 7/8 position.

The confusion matrix is a table with rows representing the true class labels and columns representing the predicted class labels. The four outcomes of the classification problem are:

- True positive (TP): the model correctly predicted the positive class.
- False positive (FP): the model incorrectly predicted the positive class.
- True negative (TN): the model correctly predicted the negative class.
- False negative (FN): the model incorrectly predicted the negative class.

Several performance metrics are calculated from these four results to show the performance of the decision tree:

- Accuracy: The proportion of correctly classified samples in the data set. It is calculated as follows:

$$\text{accuracy} = \frac{TP+TN}{(TP+TN+FP+FN)} \tag{17}$$



- Recall (also known as sensitivity): This metric indicates how well a classifier can predict a correct classification. It is calculated as follows:

$$\text{recall} = \frac{TP}{(TP+FN)} \tag{18}$$

- Precision: Precision is another important performance metric used to evaluate the performance of a classification model. Precision focuses on the proportion of correct positive predictions. It is calculated as:

$$\text{precision} = \frac{TP}{(TP+FP)} \tag{19}$$

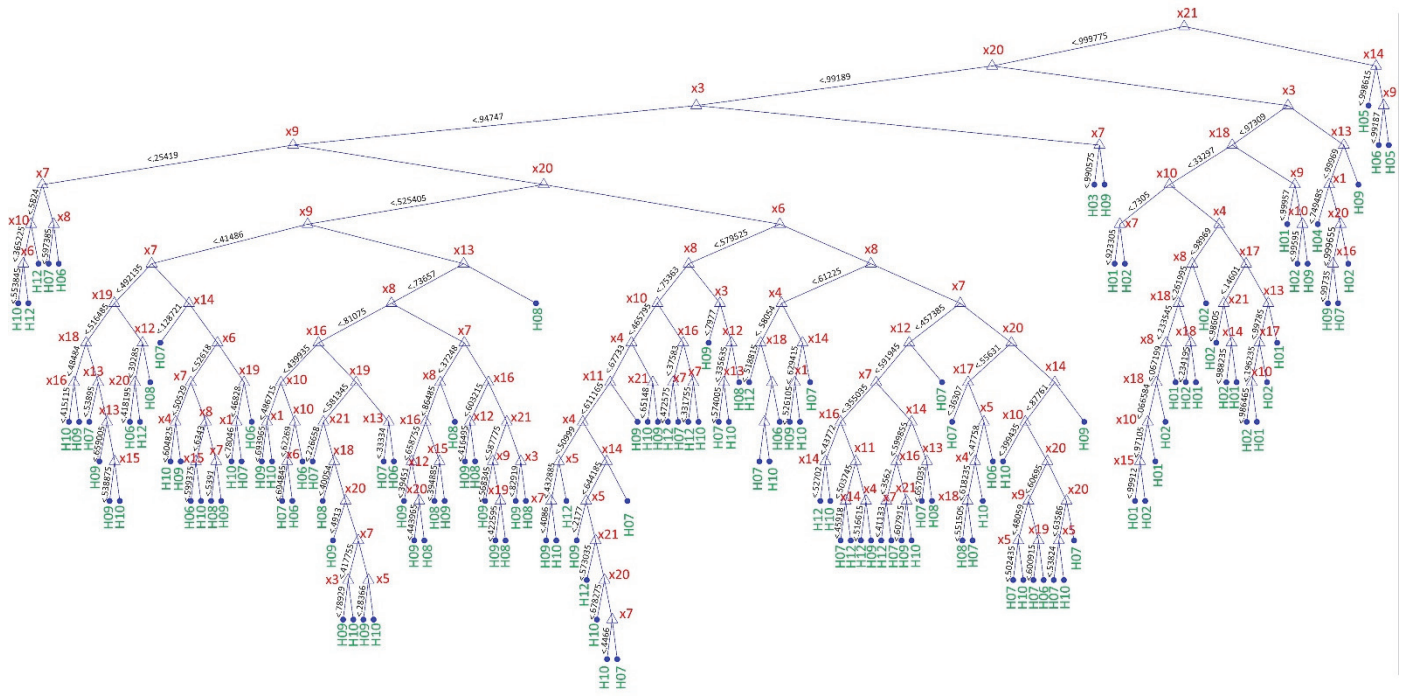


Figure 14: Decision tree model.

True Class \ Predicted Class	H01	H02	H03	H04	H05	H06	H07	H08	H09	H10	H12
H01	96.6%	1.9%									
H02	4.4%	98.1%									
H03			100.0%								
H04				98.7%							
H05				1.3%	100.0%						
H06						100.0%					
H07							100.0%				
H08								100.0%			
H09									100.0%	1.6%	
H10										98.4%	
H12											100.0%

Figure 15: The performance of classification models.

The model achieved its ability to predict almost damage instances accurately. There are several predictions by mistake at H01, H02, H05 and H09 damage scenarios, but this mistake is tiny.

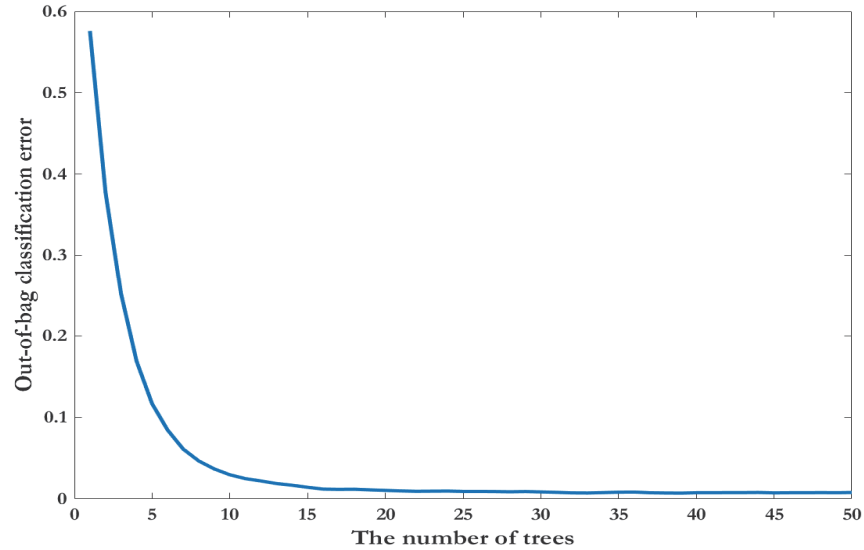


Figure 16: Out-of-bag error versus the number of trees.

According to the results shown in Fig. 16, the model's out-of-bag error tends to approach zero starting from Tree 20. The overall classification error is calculated by averaging the out-of-bag error values, which is approximately 0.043, that the model's performance is good. Based on the confusion matrix, we can calculate various evaluation metrics, such as accuracy, precision, and recall, to assess the model's performance by formulas (17), (18) and (19).

Accuracy	Recall	Precision
99.15%	94.55%	98.11%

Table 6: Several performance metrics for classification.

Based on Tab. 6, we achieved high accuracy of 99.15%, indicating that many instances were correctly classified. Furthermore, 98.11% of the optimistic predictions made by the model were accurate, indicating a high degree of precision. However, some positive instances were incorrectly classified as negatives due to the recall rate of 94.55%. Overall, these results demonstrate the effectiveness of our classification model in accurately predicting the target variable.

CONCLUSION

This article proposes a two-step diagnostic method using PSCF-based machine learning algorithms to detect damages on the beam. Based on the measurement of beam vibration data under different moving load speeds, the method is verified as a viable method to model the vibration state of a bridge deck under traffic loads. In the first step, the PSCF vectors (21 input values) at different locations are combined with an Artificial Neural Network (ANN) (consisting of two hidden layers, with each hidden layer being 25 neurons) to identify the location and appearance of damages (the output of 7 values representing the probabilities damaged of the beam). Then the PSCF vectors are used as input to the decision tree (treebagger) algorithm (50 trees) to assess the level of damage in the second step by the classification algorithm. As a result, the proposed approach can be implemented in three stages: damage detection, damage localization, and damage severity estimation.

In the proposed ANN, the factors serve as inputs and demonstrate remarkable precision. The generalizability of the ANN is confirmed based on noteworthy testing process results with an accuracy of 99.93%. Besides, the decision tree algorithm exhibits extremely accurate classification with 99.15%. However, this study must use two machine learning methods to achieve the desired results. Further research is needed to optimize the damage recognition algorithm. In addition, it is possible to create more complex damage scenarios to test the algorithm and apply it to the actual structures.



ACKNOWLEDGEMENT

This research is funded by Vietnam National University Ho Chi Minh City (VNU-HCM) under grant number C2021-20-05. We acknowledge Ho Chi Minh City University of Technology (HCMUT), VNU-HCM, for supporting this study.

REFERENCE

- [1] Rytter, A. Brincker, R., Hansen, L.P. (1993). *Vibration based inspection of civil engineering structures*. University of Aalborg, Denmark.
- [2] Rahnema, M., Vahedi, A., Alikhani, A.M. and Montazeri, A. (2019). Machine-learning approach for fault detection in brushless synchronous generator using vibration signals. *IET Science, Measurement Technology*, 13 (6), pp. 852-861. DOI: 10.1049/iet-smt.2018.5523.
- [3] Tan, Z.X., Thambiratnam, D.P., Chan, T.H., Gordan, M. and Abdul Razak, H. (2020). Damage detection in steel-concrete composite bridge using vibration characteristics and artificial neural network. *Structure Infrastructure Engineering*, 16 (9), pp. 1247-1261. DOI: 10.1080/15732479.2019.1696378.
- [4] Doebling, S.W., Farrar, C.R., Prime, M.B. and Shevitz, D.W. (1996). *Damage identification and health monitoring of structural and mechanical systems from changes in their vibration characteristics: a literature review*. U.S. Department of Energy Office of Scientific and Technical Information. DOI: 10.2172/249299.
- [5] Doebling, S.W., Farrar, C.R. and Prime, M.B. (1998). A summary review of vibration-based damage identification methods. *Shock vibration digest*, 30 (2), pp. 91-105.
- [6] Deulgaonkar, V.R. (2016). Vibration measurement and spectral analysis of chassis frame mounted structure for off-road wheeled heavy vehicles. *International Journal of Vehicle Structures Systems*, 8 (1), pp. 23. DOI: 10.4273/ijvss.8.1.05.
- [7] Pesaresi, E. and Troncosi, M., (2018). Synthesis of vibration signals with prescribed power spectral density and kurtosis value. *Proceedings of the ISMA2018 International Conference on Noise and Vibration Engineering*.
- [8] Stan, P. and Stan, M., (2017). The study spectral analysis to random vibrations for nonlinear oscillators. *International Congress of Automotive and Transport Engineering CAR*.
- [9] Zhang, F., Shengchang, J. and Lingyu, Z. (2017). Frequency response function of short circuit vibration for power transformer. *Journal of Xian Jiaotong University*.
- [10] Gurley, K. and Kareem, A. (1999). Applications of wavelet transforms in earthquake, wind and ocean engineering. *Engineering structures*, 21 (2), pp. 149-167.
- [11] Nguyen, T.Q., Vuong, L.C., Le, C.M., Ngo, N.K. and Nguyen-Xuan, H. (2020). A data-driven approach based on wavelet analysis and deep learning for identification of multiple-cracked beam structures under moving load. *Measurement*, 162, pp. 107862. DOI: 10.1016/j.measurement.2020.107862.
- [12] O'Brien, R.J., Fontana, J.M., Ponso, N. and Molisani, L. (2017). A pattern recognition system based on acoustic signals for fault detection on composite materials. *European Journal of Mechanics-A/Solids*, 64, pp. 1-10. DOI: 10.1016/j.euromechsol.2017.01.007.
- [13] Tan, Z.X., Thambiratnam, D., Chan, T. and Razak, H.A. (2017). Detecting damage in steel beams using modal strain energy based damage index and Artificial Neural Network. *Engineering Failure Analysis*, 79, pp. 253-262. DOI: 10.1016/j.engfailanal.2017.04.035.
- [14] Yaseen, Z.M., Afan, H.A. and Tran, M.-T., (2018). Beam-column joint shear prediction using hybridized deep learning neural network with genetic algorithm. *IOP conference series: earth and environmental science*, 143 (1), pp. 012025. DOI: 10.1088/1755-1315/143/1/012025.
- [15] Zhao, Q., Hao, S., Wang, Y., Wang, L., Wan, X. and Xu, C. (2018). Mode detection of misaligned orbital angular momentum beams based on convolutional neural network. *Applied Optics*, 57 (35), pp. 10152-10158.
- [16] Ngo-Kieu, N., Nguyen-Da, T., Pham-Bao, T., Nguyen-Nhat, T. and Nguyen-Xuan, H. (2021). Deep learning-based signal processing for evaluating energy dispersal in bridge structures. *Journal of Zhejiang University-Science A*, 22 (8), pp. 672-680. DOI: 10.1631/jzus.A2000414.
- [17] Pham-Bao, T., Ngo-Kieu, N., Vuong-Cong, L. and Nguyen-Nhat, T. (2022). Energy dissipation-based material deterioration assessment using random decrement technique and convolutional neural network: A case study of Saigon bridge in Ho Chi Minh City, Vietnam. *Structural Control Health Monitoring*, 29 (7), pp. e2956. DOI: 10.1002/stc.2956.



- [18] Ghandourah, E., Khatir, S., Banoqitah, E.M., Alhawsawi, A.M., Benaissa, B. and Wahab, M.A. (2023). Enhanced ANN Predictive Model for Composite Pipes Subjected to Low-Velocity Impact Loads. *Buildings*, 13 (4), p. 973.
- [19] Shirazi, M.I., Khatir, S., Benaissa, B., Mirjalili, S. and Wahab, M.A. (2023). Damage assessment in laminated composite plates using modal Strain Energy and YUKI-ANN algorithm. *Composite Structures*, 303, p. 116272.
- [20] Slimani, M., Khatir, T., Tiachacht, S., Boutchicha, D. and Benaissa, B. (2022). Experimental sensitivity analysis of sensor placement based on virtual springs and damage quantification in CFRP composite. *Journal of Materials Engineering Structures*, 9 (2), pp. 207-220.
- [21] Khatir, S., Tiachacht, S., Benaissa, B., Le Thanh, C., Capozucca, R. and Abdel Wahab, M., (2022). Damage Identification in Frame Structure Based on Inverse Analysis. *Proceedings of the 2nd International Conference on Structural Damage Modelling and Assessment: SDMA*, Ghent University, Belgium, pp. 197-211.
- [22] Benaissa, B., Hocine, N.A., Khatir, S., Riahi, M.K. and Mirjalili, S. (2021). YUKI Algorithm and POD-RBF for Elastostatic and dynamic crack identification. *Journal of computational science*, 55, pp. 101451.
- [23] Minh, H.-L., Khatir, S., Rao, R.V., Abdel Wahab, M. and Cuong-Le, T. (2023). A variable velocity strategy particle swarm optimization algorithm (VVS-PSO) for damage assessment in structures. *Engineering with Computers*, 39 (2), pp. 1055-1084.
- [24] Cuong-Le, T., Nghia-Nguyen, T., Khatir, S., Trong-Nguyen, P., Mirjalili, S. and Nguyen, K.D. (2021). An efficient approach for damage identification based on improved machine learning using PSO-SVM. *Engineering with Computers*, pp. 1-16.
- [25] Garg, A., Aggarwal, P., Aggarwal, Y., Belarbi, M., Chalak, H., Tounsi, A. and Gulia, R. (2022). Machine learning models for predicting the compressive strength of concrete containing nano silica. *Computers and Concrete*, 30 (1), pp. 33-42.
- [26] Ouladbrahim, A., Belaidi, I., Khatir, S., Magagnini, E., Capozucca, R. and Wahab, M.A. (2022). Experimental crack identification of API X70 steel pipeline using improved Artificial Neural Networks based on Whale Optimization Algorithm. *Mechanics of Materials*, 166, pp. 104200.
- [27] Tran-Ngoc, H., Khatir, S., Le-Xuan, T., De Roeck, G., Bui-Tien, T. and Wahab, M.A. (2020). A novel machine-learning based on the global search techniques using vectorized data for damage detection in structures. *International Journal of Engineering Science*, 157, pp. 103376.
- [28] He, H. and Garcia, E. (2009). Learning from Imbalanced Data *IEEE Transactions on Knowledge and Data Engineering*, 21 (9), pp. 1263-1284.
- [29] Hoshyar, A.N., Samali, B., Liyanapathirana, R., Houshyar, A.N. and Yu, Y. (2020). Structural damage detection and localization using a hybrid method and artificial intelligence techniques. *Structural Health Monitoring*, 19 (5), pp. 1507-1523.
- [30] Nazarko, P. and Ziemiański, L. (2017). Application of artificial neural networks in the damage identification of structural elements. *Computer Assisted Methods in Engineering Science*, 18 (3), pp. 175-189.
- [31] Brown, D.E., Corruble, V. and Pittard, C.L. (1993). A comparison of decision tree classifiers with back-propagation neural networks for multimodal classification problems. *Pattern Recognition*, 26 (6), pp. 953-961.
- [32] Tso, G.K. and Yau, K.K. (2007). Predicting electricity energy consumption: A comparison of regression analysis, decision tree and neural networks. *Energy*, 32 (9), pp. 1761-1768.
- [33] Newland, D.E., (2012). *An introduction to random vibrations, spectral & wavelet analysis*, Courier Corporation, United States of America.
- [34] Beskhyroun, S., Oshima, T., Mikami, S. and Tsubota, Y. (2005). Structural damage identification algorithm based on changes in power spectral density. *Journal of applied mechanics*, 8, pp. 73-84. DOI: 10.2208/journalam.8.73.
- [35] Beskhyroun, S., Oshima, T., Mikami, S., Tsubota, Y. and Takeda, T., (2006). Damage identification of steel structures based on changes in the curvature of power spectral density. *2nd International conference on structural health monitoring of intelligent infrastructure*, pp. 791-797.
- [36] Kumar, R.P., Oshima, T., Mikami, S., Miyamori, Y. and Yamazaki, T. (2012). Damage identification in a lightly reinforced concrete beam based on changes in the power spectral density. *Structure Infrastructure Engineering*, 8 (8), pp. 715-727.
- [37] Nguyen, T.D., Nguyen, H.Q., Pham, T.B. and Ngo, N.K., (2021). A novel proposal in using viscoelastic model for bridge condition assessment. *Structural Health Monitoring and Engineering Structures: Select Proceedings of SHM&ES 2020*, pp. 331-341. DOI: 10.1007/978-981-16-0945-9_27.
- [38] Pham-Bao, T., Nguyen-Nhat, T. and Ngo-Kieu, N. (2022). A novel approach to investigate the mechanical properties of the material for bridge health monitoring using convolutional neural network. *Structure Infrastructure Engineering*, pp. 1-21. DOI: 10.1080/15732479.2022.2127792.



- [39] Rodgers, J.L. and Nicewander, W.A. (1988). Thirteen ways to look at the correlation coefficient. *American statistician*, 42, pp. 59-66.
- [40] Rodríguez-Roblero, M., Ayon, J., Cascante, G., Pandey, M., Alyousef, R. and Topper, T. (2019). Application of correlation analysis techniques to surface wave testing for the evaluation of reinforced concrete structural elements. *NDT&E International*, 102, pp. 68-76. DOI: 10.1016/j.ndteint.2018.11.003.
- [41] Yan, F., Royer Jr, R.L. and Rose, J.L. (2010). Ultrasonic guided wave imaging techniques in structural health monitoring. *Journal of intelligent material Systems Structures*, 21 (3), pp. 377-384. DOI: 10.1177/1045389X09356026.
- [42] Chang, Y., Yang, D. and Guo, Y. (2018). Laser ultrasonic damage detection in coating-substrate structure via Pearson correlation coefficient. *Surface Coatings Technology*, 353, pp. 339-345. DOI: 10.1016/j.surfcoat.2018.09.005.
- [43] Zhou, Y.-L., Cao, H., Liu, Q. and Wahab, M.A. (2017). Output-based structural damage detection by using correlation analysis together with transmissibility. *Materials*, 10 (8), pp. 866. DOI: 10.3390/ma10080866.
- [44] Koyuncu, A., Cigeroglu, E. and Özgüven, H.N. (2017). Localization and identification of structural nonlinearities using cascaded optimization and neural networks. *Mechanical Systems & Signal Processing*, 95, pp. 219-238. DOI: 10.1016/j.ymsp.2017.03.030.
- [45] Nguyen, D.H., Bui, T.T., De Roeck, G. and Wahab, M.A. (2019). Damage detection in Ca-Non Bridge using transmissibility and artificial neural networks. *Structural Engineering Mechanics*, 71 (2), pp. 175-183.
- [46] Breiman, L., (2017). *Classification and regression trees*, Routledge, New York. DOI: 10.1201/9781315139470.
- [47] Lewis, R.J., (2000). *An introduction to classification and regression tree (CART) analysis*. Annual meeting of the society for academic emergency medicine in San Francisco, California.
- [48] Cutler, D.R., Edwards Jr, T.C., Beard, K.H., Cutler, A., Hess, K.T., Gibson, J. and Lawler, J.J. (2007). Random forests for classification in ecology. *Ecology*, 88 (11), pp. 2783-2792. DOI: 10.1890/07-0539.1.
- [49] Ho, T.K. (1998). The random subspace method for constructing decision forests. *IEEE transactions on pattern analysis machine intelligence*, 20 (8), pp. 832-844. DOI: 10.1109/34.709601.
- [50] Worden, K. and Dulieu-Barton, J.M. (2004). An overview of intelligent fault detection in systems and structures. *Structural Health Monitoring*, 3 (1), pp. 85-98. DOI: 10.1177/1475921704041866.
- [51] Bui-Tien, T., Bui-Ngoc, D., Nguyen-Tran, H., Nguyen-Ngoc, L., Tran-Ngoc, H. and Tran-Viet, H. (2022). Damage detection in structural health monitoring using hybrid convolution neural network and recurrent neural network. *Frattura ed Integrità Strutturale*, 16 (59), pp. 461-470. DOI: 10.3221/IGF-ESIS.59.30.
- [52] Lee, J., Kim, J., Yun, C.B., Yi, J. and Shim, J. (2002). Health-monitoring method for bridges under ordinary traffic loadings. *Journal of Sound Vibration*, 257 (2), pp. 247-264. DOI: 10.1006/jsvi.2002.5056.
- [53] Zarbaf, S.E.H.A.M., Norouzi, M., Allemang, R., Hunt, V., Helmicki, A. and Venkatesh, C. (2018). Vibration-based cable condition assessment: a novel application of neural networks. *Engineering Structures*, 177, pp. 291-305. DOI: 10.1016/j.engstruct.2018.09.060.